WOOD RESEARCH
64 (4): 2019
705-718

LASER SHOCK PROCESS AS NEW TENSIONING METHOD FOR CIRCULAR SAW BLADE

B. Li, Z. Zhang
Chinese Academy of Forestry
Research Institute of Forestry New Technology
Research Institute of Wood Industry
Beijing, China

(Received August 2018)

ABSTRACT

Laser shock process for circular saw blade was proposed and analyzed in this paper. The high pressure plasma shock wave generated by strong laser beam was applied to many local areas of circular saw blade to generate local plastic deformation. Resistance strain rosette and static strain acquisition instrument were used for measuring the stress field of laser shocked circular saw blade. The natural frequency of circular saw blade after laser shock process was tested by hammer vibration test method. Based on reasonable simplification and hypothesis, laser shock process for circular saw blade was built by finite element method. The stress field obtained by experiment and theoretical calculation shows that investigated process is feasible. The natural frequencies of laser shocked circular saw blade for nodal diameters N_d = 2 and N_d = 3 are increased which means that the dynamic stability of circular saw blade is enhanced after modification.

KEYWORDS: Circular saw blade, tensioning, laser shock.

INTRODUCTION

Circular saw blade is an important, irreplaceable and widely used tool for industry. Its stability, cutting precision and material-saving ability are the most important features, especially for wood processing industry in China because of the shortage of precious wood, as reported by Li et al. (2015a). The improvement of timber utilization is strongly supported by Chinese government in recent years, which promotes the development of circular saw blade manufacturing technology and makes circular saw blade thinner and thinner in China.

When circular saw blade is cutting work pieces, thermal stress is produced in the edge of circular saw blade because the temperature in the blade edge is higher than that in other regions. It will cause large tangential compressive stress in the edge of circular saw blade, causing buckling deformation. The deformation of circular saw blade will reduce cutting precision, increase kerf loss and shorten the saw life (Svoreň et al. 2017, Krilek et al. 2016).

Plastic deformation in many local areas of circular saw blade is produced by mechanical or other physical means, which is called tensioning. Tangential tensile stress in the edge of circular saw blade is produced after the process, which can compensate for the tangential compressive thermal stress. It is the most important process for circular saw blade and determines its quality. Li et al. (2016) pointed out that stress field produced during tensioning process is the essence and has the greatest impact on dynamic stability of saw blade. Hammering and rolling are the most widely used tensioning process. However, they have some disadvantages in effect, efficiency and automation, as reported by Li et al. (2015a).

Tensioning process and performance of circular saw blade are hot research topics and studied by many scientists. The effects of rolling parameters on stress field were examined by Heisel et al. (2014) based on ABAQUS software. The effect of yield strength of circular saw blade on stress field of rolled circular saw blade was studied by Li and Zhang (2017). Stress field of rolled circular saw blade was studied by finite element method, its effect on natural frequency and stiffness of circular saw blade was discussed by Merhar et al. (2017). An analytical model of circular saw blade was developed by Tian and Hutton (2001), which can help us understand the mechanics of lateral vibration instability. Stakhiev (2000) described the relationship between circular saw blade design, lateral stiffness and dynamic stability. Vibration mode, natural frequency and critical speed of the slotted circular saw blades are studied by Nishio and Marui (1996) based on experimental and numerical method. Orlowski et al. (2007) proposed a simple methodology for evaluation of circular saw critical rotational speed. A new design of circular saw blade with self-clamped cutting inserts is presented by Chang and Chen (2016). Chang et al. (2013) also developed an automated optical inspection (AOI) system for inspecting the run out tolerance of circular saw blade. Non-linear oscillation of circular saw blade spinning near critical speed was analyzed by Raman and Mote (2001).

Laser shock peening (LSP) process can significantly improve the fatigue life of metal parts by forming residual compressive stress in the laser shock region, as reported by Keller et al. (2018). Grain refinement can even occur on the surface of laser shock region, as reported by Huang et al. (2013). LSP can also improve the tribological performance at tribo-contacts, as reported by Mao et al. (2018). LSP is widely used in aero engine manufacturing at present, as reported by Cuellar et al. (2012). LSP has a significant advantage in efficiency, accuracy and automation, as reported by Achintha et al. (2014). Plastic deformation and residual stress field are produced during LSP as reported by Zhang et al. (2015), which is the same as tensioning process. Combination of LSP and tensioning process is interesting, scientific and creative, and can promote the development of circular saw blade. Therefore, laser shock process of circular saw blade is proposed in this paper, which is a new tensioning technology for circular saw blade and can make up the deficiency of the existing technology.

In this work, the research was focused on LSP; mainly a compressive stress in the laser shock region was investigated. However, for laser shock process, the research process is completely different. The tangential tensile stress in the region outside the impact zone and natural frequency of circular saw blade are in area of research. How the tangential stress in the edge of circular saw blade is produced after laser shock process is an interesting and valuable question, which is also an important issue in science and technology.

Principle of laser shock process of circular saw blade

Many local zones of circular saw blade are shocked by laser with high power density ($10^9 W \cdot cm^{-2}$) and short pulse (ns). Impact zones of laser shock process are also distributed in the form of axial symmetry, as shown in Fig. 1.

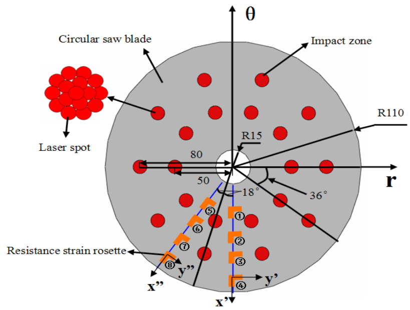

Fig. 1: The laser shock area distribution.

Plastic deformation is produced in these impact zones, which leads to the formation of stress field. Take one impact zone as example, as shown in Fig. 2, the stress state of plastic deformation zone is compressive. Around the plastic deformation zone, there are stress transition zone and tensile stress zone for maintaining the stress equilibrium of continuous media.

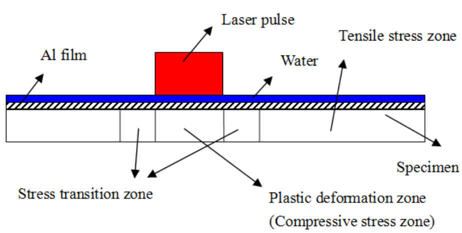

Fig. 2: Principle of laser shock process.

Sometimes, impact zone is joined by a number of laser spots for improving tensioning effect, as shown in Fig. 1. Laser spot only plays the role of extending impact zone. Therefore, the overlap ratio between laser spots is as small as possible. The distribution of laser spots in an impact zone is designed as shown below.

As shown in Fig. 3, the number of laser spots along the radial direction is *M*. It also represents the ring number of laser spot. The number of laser spots along the circumference direction of each ring is N_i, *(i = 1:M)*. To minimize the overlap ratio between laser spots along the radial direction M is shown below:

$$M = \left\lceil \frac{2R_c\text{-}D}{2D} \right\rceil + 1 \qquad (1)$$

where: Rc - is radius of impact zone (mm),
D - is diameter of laser spot (mm),
⌈ ⌉ - is rounded up operation symbols.

The distance *d* between the centres of laser spot along the radius is shown below:

$$d = \frac{R_c - 0.5D}{M - 1} \qquad (2)$$

The radius R_i of the ring of laser spot is shown below:

$$R_i = (i - 1)d, \; i = 1{:}M \tag{3}$$

To minimize the overlap ratio between laser spots of the same ring, Ni is shown below:

$$N_i = \left\lceil \frac{\pi}{\arcsin\left(D/2R_i\right)} \right\rceil, \; i = 1{:}M \tag{4}$$

α_i is the included angle as shown in Fig. 3 and shown below:

$$\alpha_i = \frac{2\pi}{N_i}, \; i = 1{:}M \tag{5}$$

Rc and D are known conditions. When M, N_i, d, R_i and α_i are determined by Eqs. 1 - 5, the positions of laser spots in an impact zone are determined. And so on, positions of laser spots in other impact zones are determined. By controlling the movement of manipulator, the specified positions for laser spots on circular saw blade are shocked in turn.

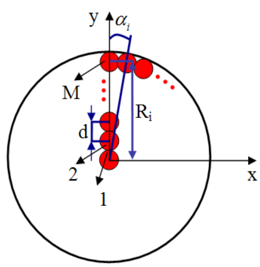

Fig. 3: Distribution pattern of laser spots.

MATERIALS AND METHODS

Circular saw blade was made from alloy spring steel GB 65Mn. Its hardness was HRC42 and dynamic yield strength was 1.29 GPa. Its outside diameter, center bore diameter and thickness were 220 mm, 30 mm and 2.2 mm, respectively.

A Nd:YAG pump laser was used, with laser energy 30 J, spot diameter 3 mm and pulse width 20 ns. Impact zone radius was 6 mm because it is necessary to reserve a certain space for resistance strain rosette. The impact zone and laser spot distribution for laser shock tensioning process are shown in Fig. 1. M, N_i, d, R_i and α_i are shown in Tab. 1.

Tab: 1: Characterization parameters for laser spot distribution of one impact zone.

M	*Ni*	*d (mm)*	R_i *(mm)*	α_i (°)
3	$N_1=1$	2.25	$R_1=0$	$\alpha_1=360$
	$N_2=5$		$R_2=2.25$	$\alpha_2=72$
	$N_3=10$		$R_3=4.5$	$\alpha_3=36$

Resistance strain rosettes (two axis, 90°) were attached to the surface of circular saw blade, as shown in Fig. 1. Resistance strain rosettes were connected to static strain acquisition instrument until the end of laser shock process. The strains of specified positions of circular saw blade in final state were recorded by static strain acquisition instrument and were shown by computer. Experimental pictures are shown in Fig. 4.

For resistance strain rosette (~) as shown in Fig. 1, stress can be described as shown below.

$$\varepsilon_r = \varepsilon_{0^\circ} \tag{6}$$

$$\varepsilon_\theta = \varepsilon_{90^\circ} \tag{7}$$

$$\sigma_r = \frac{E\left(\varepsilon_r + \mu\varepsilon_\theta\right)}{1-\mu^2} \tag{8}$$

$$\sigma_\theta = \frac{E\left(\mu\varepsilon_r + \varepsilon_\theta\right)}{1-\mu^2} \tag{9}$$

where: $\mathcal{E}_{0^\circ}$ and $\mathcal{E}_{90^\circ}$ are the strain of resistance strain rosette,
$\mathcal{E}_r$ and $\mathcal{E}_\emptyset$ are radial and tangential strain,
$\mathcal{E}_r$ and $\mathcal{E}_\emptyset$ are radial and tangential stress (MPa),
E - Elastic modulus of circular saw blade equals 210 GPa,
μ - Poisson's ratio of circular saw blade equals 0.3,
$\mathcal{E}_{0^\circ}$ and $\mathcal{E}_{90^\circ}$ of points (~) of circular saw blade in final state were tested by resistance strain rosette.

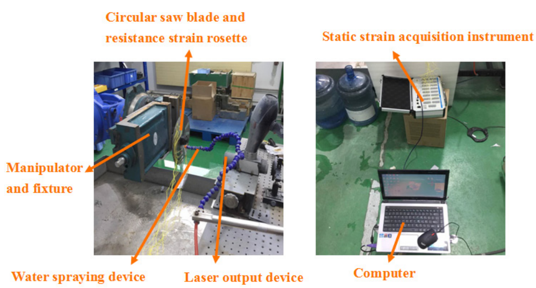

Fig. 4: Experimental pictures.

The natural frequency of circular saw blade before and after laser shock process was tested by hammer vibration test method, as shown in Fig. 5. For natural frequency test of circular saw blade before and after laser shock process, the impact zone radius was 6, 9 and 12 mm.

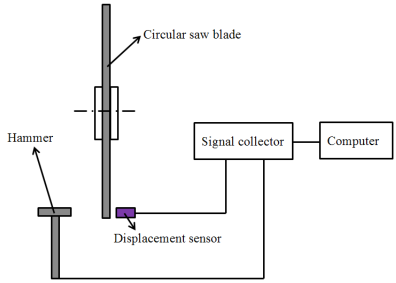

Fig. 5: Experimental pictures.

Establishment of theoretical model

Simplified mechanical model for laser shock process

Direct modelling for laser shock process of circular saw blade based on finite element method needs very large computing resources, which leads to very low computational efficiency. According to the mechanism of elastoplastic deformation of laser shock process, three assumptions were made for building its theoretical model.

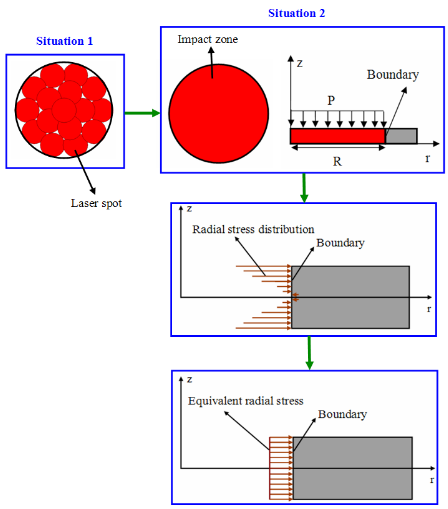

Fig. 6: Simplification of mechanical model of laser shock process.

As shown in Fig. 6, situation 1 and 2 were approximately equivalent and had the same shock wave pressure. The lapping process of laser spots was not considered and simulated in this paper. Although the outer edge of actual impact zone is not the ideal circle and the actual impact zone area is slightly smaller than circular area, the overlapping process of laser spots can compensate for this difference to some extent. Therefore, the above hypothesis has scientific support and engineering significance.

The impact zone of circular saw blade was replaced by a through-hole. The inner wall of the through-hole was subjected to equivalent radial stress, as shown in Figs. 6 and 7. The stress field obtained by the above-mentioned model was approximately equivalent to the tensioning stress field.

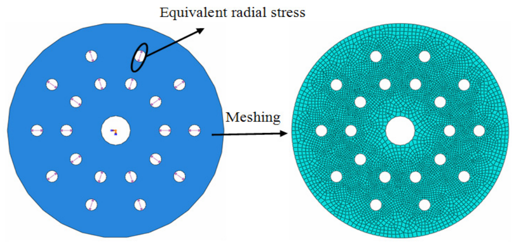

Fig. 7: Mechanical model of circular saw blade with through-holes.

Theoretical calculation of shock wave pressure

The peak pressure Pmax of laser shock wave is given by Ding and Ye (2006), Ding (2013), as shown below:

$$P_{\max} = 0.01\left(\frac{\alpha}{2\alpha+3}\right)^{0.5} Z^{0.5} I_0^{\ 0.5} \tag{10}$$

Where, α is the efficiency of the interaction, it was also reasonably assumed that 10% (α=0.1) of the incident energy density is used for the pressure rise of the plasma, as report Peyre et al. (1996). Z is the reduced acoustic impedance, g·cm^{-2}·s^{-1}. I_0 is laser power density, (GW·cm^{-2}).

Laser power density I0 is expressed by the following formula:

$$I_0 = \frac{4E}{\pi d^2 \tau} \tag{11}$$

where: E - is laser energy (J),
d - is laser spot diameter (mm),
τ - is laser pulse width (ns).

The reduced acoustic impedance Z is expressed by the following formula:

$$Z = 2\frac{Z_{target} Z_{water}}{Z_{target} + Z_{water}} \tag{12}$$

where: Z_{water} - is the acoustic impedance of water,
Z_{water} = 0.165 x 106 g·cm^{-2}·s^{-1},
Z_{target} - is the acoustic impedance of 65Mn, $Z_{target} = \rho D$,
ρ - density of 65Mn, ρ= 7.8 g·cm^{-3},
D - the shock wave velocity, D=5200 cm·s^{-1},
Z_{target} = 4.056 x 106 g·cm^{-2}·s^{-1}.

The related parameters of laser were shown in Tab. 2. The peak pressure P_{max} calculated by Eqs. 10-12 is 4.58 GPa. In the whole period of laser shock process, the shock wave pressure presents a quasi Gauss distribution which increases first and then decreases. The shock wave loading time is usually 2-3 times of the laser pulse width, as reported by Achintha and Nowell (2011). The curve of shock wave pressure versus time was shown in Fig. 8.

Tab. 2: Related parameters of laser in this paper.

Parameter	Laser energy (J)	Laser spot diameter (mm)	Laser pulse width (ns)
Value	30	3	20

Establishment of nonlinear element model

Based on ABAQUS software, an axially symmetrical model was built for simulating one impact zone laser shock process. Its unloading process was simulated by Static/General solution module using the stress field of loading process as initial conditions.

The material model of circular saw blade was set as ideal elastic-plastic model, based on the research of Hfaiedh et al. (2015). Dynamic yield strength of circular saw blade was set to 1.29 GPa. Poisson's ratio, elastic modulus and density of circular saw blade were set as 0.3, 210 GPa and 7.8 g·cm^{-3}, respectively. Half thickness of circular saw blade was 1.1 mm.

Symmetry constraint in z direction was applied to the symmetry plane in thickness direction of circular saw blade, as shown in Fig. 8. Shock wave pressure load were applied to impact zone, with peak pressure 4.58 GPa. The 4-node bilinear axisymmetric quadrilateral element CAX4R was chosen for circular saw blade.

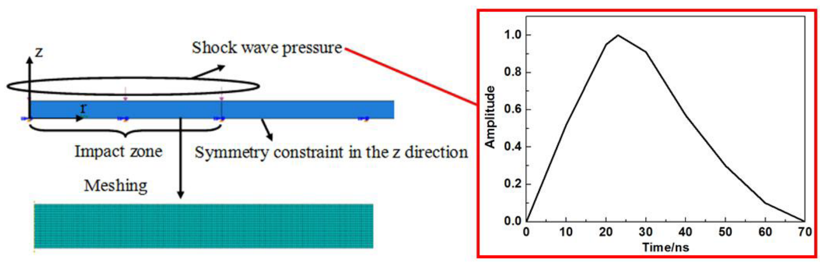

Fig. 8: Finite element model for one impact zone during laser shock process.

A plane stress finite element model was built, as shown in Fig. 7. Displacement fixed constraint was applied to the inner wall of the center hole of circular saw blade. The equivalent radial stress applied to the inner wall of the through-hole was obtained by the finite element model as shown in Fig. 8. The radius of through-hole (radius of impact zone) was set as 6 mm. The 4-node bilinear plane stress quadrilateral element CPS4R was chosen for the circular saw blade.

RESULTS

Tangential stress field is shown in Fig. 9.

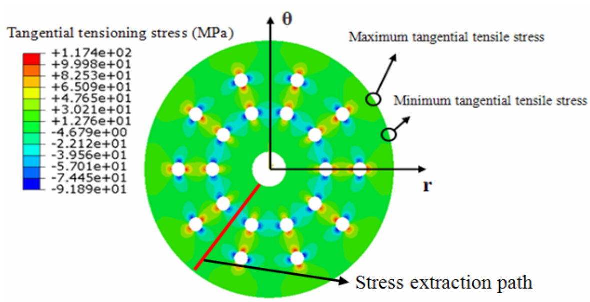

Fig. 9: Tangential tensioning stress field of circular saw blade.

Radial and tangential tensioning stresses of positions in Fig. 1 were tested. Simulated radial and tangential tensioning stresses were extracted from the path in Fig. 9. Simulation results and experimental results were shown in Fig. 10.

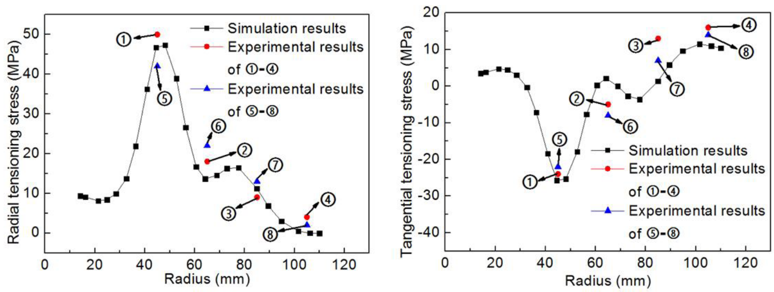

(a) Radial tensioning stress. *(b) Tangential tensioning stress.*
Fig. 10: Contrast of tensioning stress between simulation and experimental results.

Relationship between size of impact zone and tensioning stress field of circular saw blade is shown in Fig. 11.

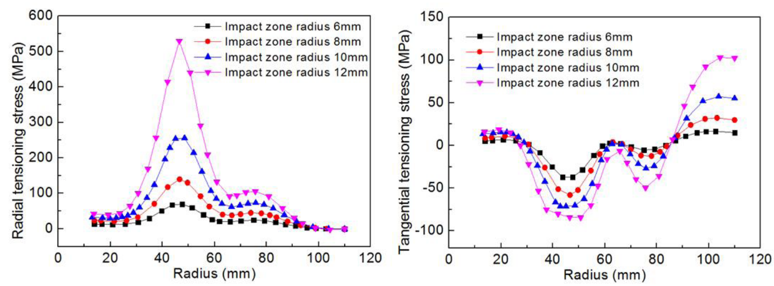

(a) Radial tensioning stress. *(b) Tangential tensioning stress.*
Fig. 11: Tensioning stress distribution with different impact zone radius.

Natural frequency of circular saw blade after laser shock tensioning process was as shown in Tab. 3.

Tab. 3: Natural frequency of m=0, n=2 and m=0, n=3, unit: Hz.

Vibration mode / Impact zone radius (mm)	m=0, n=2	m=0, n=3
0	410	623
6	422	639
9	443	673
12	476	705

DISCUSSION

Tensioning stress analysis of circular saw blade

As shown in Fig. 9, taking the center of circular saw blade as the origin of polar coordinate, tensioning stress of the region outside impact zones has a cyclic axisymmetric distribution. Tensioning stress field of circular saw blade after laser shock process has same distribution form as multi-spot pressure tensioning process, as reported by Li et al. (2015a) and Li et al. (2015b). Maximum and minimum tangential tensile stresses were marked in Fig. 9, which appear alternately in the circumferential direction of outer edge of circular saw blade. The impact zones with axisymmetric distribution make the stress in the edge of circular saw blade approximately equal. It keeps the stress state in different position of circular saw blade unchanged during sawing.

In this experiment, the maximum depth of impact zone is about 45 μm. For finite element model, the calculated maximum depth of impact zone is 42 μm. The error between them is acceptable. This result also shows that plastic deformation is produced in the impact zone during laser shock process.

As shown in Fig. 10, simulation results were in good agreement with the experimental results. It is noteworthy that tangential tensile stress is produced in the edge of circular saw blade after laser shock process, which is an important sign of tensioning effect. Radial tensile stress is produced in the path of Fig. 9, which can also improve the dynamic stability of circular saw blade. Radial compressive stress is produced during roll tensioning process, which is not beneficial for dynamic stability of circular saw blade, as reported by Li and Zhang (2017). Plastic deformation is produced in the impact zones. The outward expansion effect of impact zones is constrained by the surrounding elastic deformation zone. It leads to the generation of tensile stress in the surrounding elastic deformation zone.

Meanwhile, the tangential tensile stress is increased with radius in the edge of circular saw blade, which is a favourable distribution form. The distribution form of plastic deformation zones determines the distribution of tensioning stress. The experimental results not only proved the correctness of the simulation model, but also illustrated the feasibility of laser shock process. Although laser shock process has not yet been applied, the research results of this paper are important technical reserves for future promotion of this technology.

In this experiment, the tangential tensile stress in the edge of circular saw blade is about 10 MPa, which is relatively small. The reason is that the impact zone is small. The stress zone is formed in the impact zone and it has a small range of influence because of Saint Venant principle in elastic mechanics. The impact zone radius in this experiment was only 6 mm because it is necessary to reserve a certain space for resistance strain rosette. If there is not enough space for resistance strain rosette, laser shock wave will hit resistance strain rosette. It will seriously affect the accuracy of the test. The impact zone can be enlarged easily by adjusting the running track of manipulator. When the size of impact zone is enlarged, the tangential tensile stress in the edge of saw blade is further increased, as shown in Fig. 11.

When the size of impact zone is enlarged, the stress zone formed in the impact zone is also enlarged. It has a large range of influence because of Saint Venant principle in elastic mechanics. As shown in Fig. 11, the tangential tensile stress in the edge of circular saw blade is increased from 10 MPa to 105 MPa when impact zone radius is increased from 6 mm to 12 mm. It means that the outer edge of circular saw blade is tightened and it can better counteract the thermal stress during cutting process. Circular saw blade with tightened outer edge can also reduce its vibration when circular saw blade is cutting material. Tensioning stress field produced by laser shock tensioning process is the core factor which can improve the comprehensive performance of circular saw blade.

Natural frequency analysis of circular saw blade

Critical speed is increased with natural frequency of circular saw blade in static state, as reported by Orlowski et al. (2007). Based on the predecessor's research, natural frequencies of m=0, n=0 and m=0, n=1 are close. Below 2000 Hz, nodal circle m is usually 0 because it needs a lot of energy to excite the vibration mode of m>0. Below 2000 Hz, natural frequency of circular saw blade is increased with nodal diameter n. Spectrum analysis diagram of circular saw blade shown in this paper conforms to the theory of previous studies, as reported by Schajer and Mote (1983).

Natural frequency of circular saw blade is changed after laser shock process, as shown in Tab. 3. It is due to the stress field produced during laser shock process. Natural frequency of circular saw blade is increased after laser shock process. It means that critical speed of circular saw blade is increased. When circular saw blade is cutting material, natural frequency of circular saw blade will decline because of the accumulation of thermal stress. If natural frequency of circular saw blade is increased before circular saw blade is used, circular saw blade can maintain stable working condition for a longer time.

As shown in Tab. 3, natural frequency for m=0, n=2 is increased from 410 Hz to 476 Hz and natural frequency for m=0, n=3 is increased from 623 Hz to 705 Hz, when impact zone radius is increased from 0 mm to 12 mm. It means that circular saw blade can maintain stable working condition for a long time after laser shock process. The increase amplitude of natural frequency relative to the un-tensioned circular saw blade is increased with impact zone radius.

Combined with the stress analysis of circular saw blade after laser shock process, impact zone radius is important for the performance improvement of circular saw blade. If circular saw blade has no obvious macroscopic deformation after laser shock process, the bigger the impact zone radius, the better.

CONCLUSIONS

(1) Laser shock process of circular saw blade is proposed in this paper. A reasonable stress field is generated in the saw blade after modification, which is proved to be true by stress test experiment and simulation.
(2) Simulation and experimental results show that the radial stress outside the impact zones is tensile stress and the tangential tensile stress increases with radius in the edge area of circular saw blade, which is favourable to the stability of this cutting tool.
(3) Natural frequency of circular saw blade is increased after laser modification, which means that cutting tool can be maintained stable at working conditions for a longer time.

ACKNOWLEDGEMENTS

We gratefully acknowledge to the financial support of Fundamental Research Funds for the Central Non-profit Research Institution of CAF (No.CAFYBB2019QB006, CAFYBB2017SY039) and National Natural Science Foundation of China (No.31600458).

REFERENCES

1. Achintha, M., Nowell, D., 2011: Eigen strain modelling of residual stresses generated by laser shock peening. Journal of Materials Processing Technology 211(6): 1091-1101.
2. Achintha, M., Nowell, D., Fufari, D., Sackeet, E.E., Bache, M.R., 2014: Fatigue behavior of geometric features subjected to laser shock peening: Experiments and modeling. International Journal of Fatigue 44: 171-179.
3. Chang, W.T., Chen, L.C., 2016: Design and experimental evaluation of a circular saw blade with self-clamped cutting inserts. The International Journal of Advanced Manufacturing Technology 83(1-4): 365-379.
4. Chang, W.T., Su, C.H., Guo, D.X., Tang, G.R., Shiou, F.J., 2013: Automated optical inspection for the run out tolerance of circular saw blades. The International Journal of Advanced Manufacturing Technology 66(1-4): 565-582.
5. Cuellar, S.D., Hill, M.R., De Wald, A.T., Rankin, J.E., 2012: Residual stress and fatigue life in laser shock peened open hole samples. International Journal of Fatigue 44: 8-13.
6. Ding, K., Ye, L., 2006: Simulation of multiple laser shock peening of a 35CD4 steel alloy. Journal of Materials Processing Technology 178(1-3): 162-169.
7. Ding, K., 2013: Three-dimensional dynamic finite element analysis of multiple laser shock peening processes. Surface Engineering 19(5): 351-358.
8. Heisel, U., Stehle, T., Ghassemi, H., 2014: A simulation model for analysis of roll tensioning of circular saw blade. Advanced Materials Research 1018: 57-66.
9. Hfaiedh, N., Peyre, P., Song, H., Popa, L., Ji, V., Vignal, V., 2015: Finite element analysis of laser shock peening of 2050-T8 aluminum alloy. International Journal of Fatigue 70: 480-489.
10. Huang, S., Zhou, J.Z., Sheng, J., Luo, K.Y., Lu, J.Z., Xu, Z.C., Meng, X.K., Dai, L., Zuo, L.D., Ruan, H.Y., Chen, H.S., 2013: Effects of laser peening with different coverage areas on fatigue crack growth properties of 6061-T6 aluminum alloy. International Journal of Fatigue 47(2): 292-299.
11. Keller, S., Chupakhin, S., Staron, P., Maawad, E., Kashaev, N., Klusemann, B., 2018: Experimental and numerical investigation of residual stresses in laser shock peened AA2198. Journal of Materials Processing Technology 255: 294-307.
12. Krilek, J., Kovac, J., Barcik, S., Svoren, J., Stefanek, M., Kuvik, T., 2016: The influence of chosen factors of a circular saw blade on the noise level in the process of cross cutting wood. Wood Research 61(3): 475-486.
13. Li, B., Zhang, Z.K., Li, W.G., Peng, X.R., 2015a: A numerical simulation on multi-spot pressure tensioning process of circular saw blade. Journal of Wood Science 61(6): 578-585.
14. Li, B., Zhang, Z.K., Li, W.G., Peng, X.R., 2015b: Model for tangential tensioning stress in the edge of circular saw blades tensioned by multi-spot pressure. BioResources 10(2): 3798-3810.
15. Li, B., Zhang, Z.K., 2017: Research on the effect of yield strength of circular saw blade on roll tensioning process. Journal of Wood Science 63(2): 140-146.
16. Li, S., Wang, C., Zheng, L., Wang, Y., Xu, X., Feng, D., 2016: Dynamic stability of cemented carbide circular saw blades for woodcutting. Journal of Materials Processing Technology 238: 108-123.
17. Mao, B., Siddaiah, A., Menezes, P.L., Liao, Y., 2018: Surface texturing by indirect laser shock surface patterning for manipulated friction coefficient. Journal of Materials Processing Technology 257: 227-233.

18. Merhar, M., Bučar, D.G., Pepelnjak, T., 2017: Dynamic behaviour analysis of a commercial roll-tensioned circular saw blade. Bioresources 12(3): 5569-5582.
19. Nishio, S., Marui, E., 1996: Effects of slots on the lateral vibration of a circular saw blade. International Journal of Machine Tools and Manufacture 36(7): 771-787.
20. Orlowski, K., Sandak, J., Tanaka, C., 2007: The critical rotational speed of circular saw: simple measurement method and its practical implementations. Journal of Wood Science 53(5): 388-393.
21. Peyre, P., Fabbro, R., Merrien, P., Lieurade, H.P., 1996: Laser shock processing of aluminium alloys. Application to high cycle fatigue behavior. Materials Science and Engineering A 210(1-2): 102-113.
22. Raman, A., Mote, C.D., 2001: Effects of imperfection on the non-linear oscillations of circular plates spinning near critical speed. International Journal of Non-Linear Mechanics 36(2): 261-289.
23. Schajer, G.S., Mote, C.D., 1983: Analysis of roll tensioning and its influence on circular saw stability. Wood Science and Technology 17(4): 287-302.
24. Stakhiev, Y.M., 2000: Today and tomorrow circular saw blades: Russian version. Holz als Roh- und Werkstoff 58(4): 229-240.
25. Svoreň, J., Javorek, Ľ., Krajčovičová, M., Klobušiaková, M., Kubovský, I., Kminiak, R., 2017: The effect of the circular saw blade body structure on the concentric distribution of the temperature along the radius during the wood cutting process. Wood Research 62(3): 427-436.
26. Tian, J.F., Hutton, S.G., 2001: Cutting-induced vibration in circular saws. Journal of Sound and Vibration 242(5): 907-922.
27. Zhang, X., She, J., Li, S., Duan, S., Zhou, Y., Yu, X., Zheng, R., Zhang, B., 2015: Simulation on deforming progress and stress evolution during laser shock forming with finite element method. Journal of Materials Processing Technology 220: 27-35.

B. Li*, Z. Zhang
Chinese Academy of Forestry
Research Institute of Forestry New Technology
Research Institute of Wood Industry
Beijing 100091
China
*Corresponding author: libohongxing@sina.com
Phone: +0086-10-62889443